Chemical Engineering Journal 264 (2015) 945–953

Contents lists available at ScienceDirect

Chemical Engineering Journal

journal homepage: www.elsevier.com/locate/cej

Gas distribution of a downward micro-nozzle assisted fluidized bed of fine powder

Xiaogang Yang, J. Ruud van Ommen, Robert F. Mudde *

Department of Chemical Engineering, Delft University of Technology, Julianalaan 136, 2628BL Delft, The Netherlands

HIGHLIGHTS

- We study the gas distribution in a downward micro-nozzle assisted fluidized bed.
- Time-resolved measurements are done with a high speed X-ray tomography.
- The gas flow pattern below the nozzle is analyzed.
- We find a void surrounded by diluted area, and a compacted area near the bed wall.
- Correlation of the penetration depth of the gas jet is carried out.

GRAPHICAL ABSTRACT

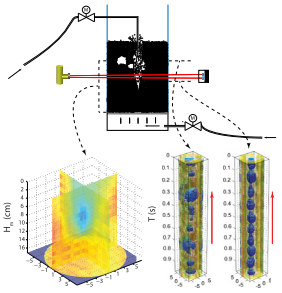

ARTICLE INFO

Article history:
Received 26 May 2014
Received in revised form 25 November 2014
Accepted 26 November 2014
Available online 4 December 2014

Keywords:
Downward micro-nozzle
Fine powder
Fluidized bed
High speed X-ray tomography

ABSTRACT

A downward micro-nozzle system is investigated for the fluidization of fine particles. To study the impact of the gas flow from the nozzle on the fluidization, the gas distribution below the nozzle is measured in a bed filled with 76 μm Puralox particles. A high speed X-ray tomography system, consisting of 3 X-ray sources and 2 layers of 32 detectors for each source, is employed to visualize the gas distribution with a temporal resolution of 2500 fps. Both the time-averaged and time resolved results are analyzed by combining the tomographic images from different measurement heights. A bubbling area, diluted area, and compacted area are found from the time averaged results. From time-series analysis, a stable bubbling flow is detected from both the cross-correlation of the raw data and image reconstruction. The penetration depth is also estimated. The results are validated with correlations from literature.

1. Introduction

A downward micro-nozzle system is a device to assist the fluidization by adding a second gas input via the nozzle for an additional shear force. There are two main features of this system: a downward gas flow from the nozzle, and a high gas injection velocity of the nozzle. Downward jets in 2-D fluidized beds have been studied by Shen et al. [1] and simulated by Hong et al. [2]. Better mixing and contacting of gas and solid is concluded from their research. In the study of a high velocity gas jet in a fluidized bed, Li et al. [3] suggest that a higher throughput is achieved at a low gas flow rate. Quevedo et al. [4] proposed a downward micro-nozzle system to enhance the fluidization of nano-particles.

Fluidization of nano-particles is often hampered by agglomeration problems, which make the gas–solid contacting inhomogeneous. Techniques such as mechanical vibration [5], sound vibration [6], alternating electric fields [7], and flow pulsation [8] have been developed to break the agglomerates. Alternatively, a downward micro-nozzle [9] was proposed to solve this problem. It is simple and works with only gas flow. Additional forces are not required, making it promising for industrial application. However, voidage distribution in such a system has not yet been

* Corresponding author. Tel.: +31 15 278 2834.
E-mail addresses: xiaogang.yang@tudelft.nl (X. Yang), R.F.Mudde@tudelft.nl (R.F. Mudde).

http://dx.doi.org/10.1016/j.cej.2014.11.127
1385-8947/

studied. The impact area and the flow pattern of the gas jet from the nozzle is difficult to predict. Direct observation of the gas–solid flow with a downward micro-nozzle has not been done. The conditions for fluidization of the nano-particles is rather difficult. To make an easy and equivalent observation for agglomerated nano-particles, we study a downward micro-nozzle assisted fluidized bed filled with a Geldart A particle.

In this paper, measurements of the dynamic flow pattern for a downward micro-nozzle system are carried out. Powders with mean size of 76 μm are used. We keep the fluidized bed at minimum fluidization and inject the gas through the micro-nozzle, which allows us to observe the influence from the nozzle only. A high speed X-ray tomography system [10,11] is applied to scan the solid fraction distribution at several cross sections below the nozzle. We reconstruct 3-D images of the solid fraction to study the bed volume below the nozzle that is influenced by the gas coming from the nozzle. We reconstruct time-resolved pseudo 3-D images to show the gas flow through specific cross sections. The gas-particle flow pattern below the nozzle is discussed. To validate these measurements, the penetration depths of the jet in the fluidized bed is compared with correlations from literature.

2. Experimental setup

2.1. The downward micro-nozzle system

The fluidized bed is held in a 14 cm inner diameter tube (perspex, wall thickness 5 mm). There are two gas inlets: a downward facing micro-nozzle and a distribution plate. The micro-nozzle is inserted from the top of the bed. It is directed downwards along the vertical axis of the bed. Its inner diameter at the outlet is 1.6 mm. The distribution plate which also supports the particles, is a porous plate made from sintered bronze. The pore size is 30–70 μm and its thickness is 7 mm.

The column is filled up to a height of 45 cm with Puralox particles, with a mean diameter of 76 μm. The powder is Geldart type A. The bulk density is 1.29×10^3 kg/m^3. The mean density of packed Puralox is 710 kg/m^3. The solid fraction of a packed bed is 0.55. In one set of experiments, we use tap water instead of particles in the same column.

The gas flows are provided by the distribution plate and micro-nozzle, respectively. The gas flow from the distribution plate keeps the particles at minimum fluidization condition: $U_{mf} = 0.21$ cm/s. The micro-nozzle provides an additional gas flow with a gas velocity at the nozzle exit ranging from 0.8×10^2 m/s to 3.3×10^2 m/s. Two digital mass flow controllers (Bronkhorst E-7100-AAA) are used to set the gas flow rate, with a maximum error of 2%.

For the different nozzle diameters, we have prepared 4 sizes: 1.6 mm, 0.8 mm, 0.4 mm, 0.2 mm. With the maximum gas supply (7 bar) in our lab, we cannot detect the difference from the X-ray measurement compared to the case without gas injection for the 0.4 mm and 0.2 mm nozzle. Apparently, the gas flow from these nozzles is too small to form a gas jet in the fluidized bed. For the 0.8 mm nozzle, the gas flow of the nozzle is only stable when the flow rate is smaller than 10 L/min. It is very difficult to obtain series of data to compare with the 1.6 mm nozzle. So we only present results of the 1.6 mm nozzle in this article.

2.2. High speed X-ray tomography

The high speed X-ray tomography system developed by Mudde et al. [10] has been applied earlier for bubbling fluidized bed measurements [12–14]. It has been shown that this system is able to measure individual bubbles with an equivalent diameter larger than 2 cm in a fluidized bed of 24 cm diameter. For measuring the 14 cm fluidized bed in the current paper, the distance between X-ray sources and detector arrays are decreased. In this way, the concentration of the X-ray projection in the cross section of the bed is increased. As a consequence, gas voids which are larger than 1 cm can be detected with the current system.

In medical X-ray CT, the source and detector combination rotates slowly around the patient. This way sufficient viewing angles are gathered for a reconstruction with high spatial resolution. However, typically the rotation speed is 3 rounds per second which is way too low for studying dynamic phenomena such as bubble motion. Therefor, we use a high speed X-ray tomographic system that is composed of 3 X-ray tubes and 3 detector arrays. The X-ray sources are placed at 120° around the fluidized bed. The detector arrays are placed opposite to the X-ray sources. There are 2 parallel layers (10.8 mm apart) of 32 detectors placed as arches in each detector array. Fig. 1(b) shows the X-ray source and detector array. As is illustrated in Fig. 1(c), this design makes it possible to simultaneously obtain the X-ray attenuation data from different directions, enabling reconstruction of the image of the object's cross section.

The X-ray sources are X-ray tubes manufactured by Yxlon International GmbH, with a maximum energy of 150 keV. The tubes currents are set at 2 mA in the present measurements. The detectors are $CdWO_4$ scintilation detectors which are manufactured by Hamamatsu (type: S 1337-1010BR). The crystal size of the detector is 10 mm × 10 mm × 10 mm. The detectors are connected to a micro-computer to synchronize the data from all the detector arrays, with a sampling frequency of 2500 Hz. After each measurement, the data are transferred to a data acquisition workstation.

3. Tomographic reconstruction

3.1. Calibration

The measured data is the X-ray intensity. We use the intensity difference to determine the attenuation difference of the X-ray traveled through different length of the object material. Mudde et al. [10] applied an exponential function to calculate the equivalent length (x, mm) of the X-ray traveled through the solid phase, from the X-ray intensity (I). In the current study, we found that a higher accuracy can be obtained by directly fitting the inversed function. It becomes:

$$x = C_{cal} \ln\left[\frac{B_{cal}}{I - A_{cal}}\right] \tag{1}$$

Here A_{cal}, B_{cal}, and C_{cal} are calibration coefficients. We fill 6 different parts of the cross sectional area, in order to have 6 specific values of x for each detector. After the related I is measured, A_{cal}, B_{cal}, and C_{cal} can be fitted from x and I in a calibration step for each detector individually.

3.2. Reconstruction process

We use a uniform Cartesian mesh to divide the computing domain in pixels. In the reconstruction, we estimate the solids volume fraction in each pixel. The values are stored in a vector (see Fig. 2) rather than a matrix for computational reasons. When a given X-ray travels through the fluidized bed, it intersects a known length through each pixel of the mesh. All these lengths form the weighting matrix **W**. The solid fraction α_j is obtained by solving:

$$\tilde{p}_i = \sum_{j=1}^{N} W_{ij}\alpha_j \tag{2}$$

where $\tilde{p}_i$ is the ith ray sum, which is the fraction of the line traveled by the ith beam occupied by solids; W_{ij} is the weighting factor for